# Analytic solution of phreatic surface in the slope of reservoir bank

Tang Xiaosong[1], Zheng Yingren[1], Shi Weimin[2]

(1. Department of Architecture & Civil Engineering, LEU, Chongqing 400041, China;
2. Institute of Engineering Designing, Military District of Lanzhou, Lanzhou 730000, China)

**Abstract**: In most cases, the slope stability of reservoir bank is analyzed on the premise that the location of phreatic surface is obtained. But many designers generalize a line as the phreatic surface through their experience to analyze the stability, which is unsafe in the project. To find a solution of the phreatic surface which is convenient to put into use and in accordance with the practice, the article, based on Boussinesq equation, infers analytic solutions suitable to the water level at different ratios and achieves an analytic solution equation through fitting curves. The correctness of the equation is also proved by the experiments of sand and sand-clay models and the inaccuracy of empirical generalization is analyzed quantitatively. The calculation results show that the inaccuracy through the method of experiential generalizing is so large that the designers should be awake to it.

**Key words**: reservoir banks; phreatic surface; analytic solution; numerical solution; empirical generalization

## 1 Introduction

At present many researches on the analytic solution of phreatic surface are conducted in dam constructions[1-3]. Since the phreatic surface in the dam is comparatively not very slanting, it can be simplified as one dimension and obtained through Boussinesq equation. This method can be used in specified structural style and boundary condition, but is not suitable to the slope of reservoir bank.

Some experts adopted the methods mentioned above to research the analytic solution of phreatic surface in the slope of reservoir bank[4-7]. Shi Weimin simplifies the problem as a one dimension unstable seepage through Boussinesq equation and obtains the analytic solution through Laplace transformation equation. While establishing the mathematical model, it is assumed that the water level changes at a constant speed. But in fact, the water level fluctuates and cascades continually. The water level seldom changes at a constant speed. So the further studies on the analytic solution of phreatic surface in the slope of reservoir bank are necessary.

## 2 The derivation of analytic solution of phreatic surface in the slope of reservoir bank

### 2.1 Basic equations

The following are premises before the derivation of the analytic solution:

1) The water bearing layer is isotrope and the side direction extends unlimitedly which is above the horizontal confiningbed. The inflow of the upper boundary can be ignored.

2) The initial phreatic surface is horizontal and hydraulic gradient is zero before the change of reservoir water level.

3) The water level rises or descends instantaneously by $\Delta h_{0,t} = h_{0,t} - h_{0,0}$ and it remains constant after the change.

4) The seepage is a one dimensional flow.

From the premises, we can find that the water level is assumed to change in the period of $\Delta t$ by $\Delta h_i$ instead of at a constant velocity (if water ascends, $\Delta h_i > 0$; if water descends, $\Delta h_i < 0$; if water remains still, $\Delta h_i = 0$). As a result, if $\Delta t$ (the time during which $\Delta h_i$ takes place) is split, the water level change velocity can be illustrated through this method.

The flow of underground water in the above situation can be described by Boussinesq equation. The differential equation under no inflow condition is:

$$\frac{\partial h}{\partial t} = \frac{k}{\mu}\frac{\partial}{\partial x}\left(h\frac{\partial h}{\partial x}\right) \quad (1)$$

It is a second-order nonlinear partial differential equation which has no analytic solution at present. So it should be simplified and linearized. By approximating $h$ in Eq. (1) to a numeric constant, it can be replaced by the average thickness of water bearing layer

*Received* 23 *January* 2008

$h_m$ and moved outside the sign of differentiation on the premises that the change of water level $\Delta h$ is less than $0.1h$ ($h$ is the thickness of water bearing layer)[8]. So Eq. (1) can be linearized as:

$$\frac{\partial h}{\partial t} = a\frac{\partial^2 h}{\partial x^2},\ a = \frac{kh_m}{\mu} \tag{2}$$

This method is called the first linearization of Boussinesq equation. The choosing of calculation coordinates is showed in Fig. 1. In the beginning, $t = 0$, the initial height of phreatic surface is $h_{0,0}$, which is showed in the second premise. The amplitude of phreatic surface at the section of the time $t$ can be shown in the following equation. ($x$ is the section's distance from the original calculation point)

$$u(x,t) = h_{x,t} - h_{0,0} = \Delta h_{x,t} \tag{3}$$

The amplitude of phreatic surface at the section of $t = 0$ is

$$u(x,0) = h_{x,0} - h_{0,0} = 0 \tag{4}$$

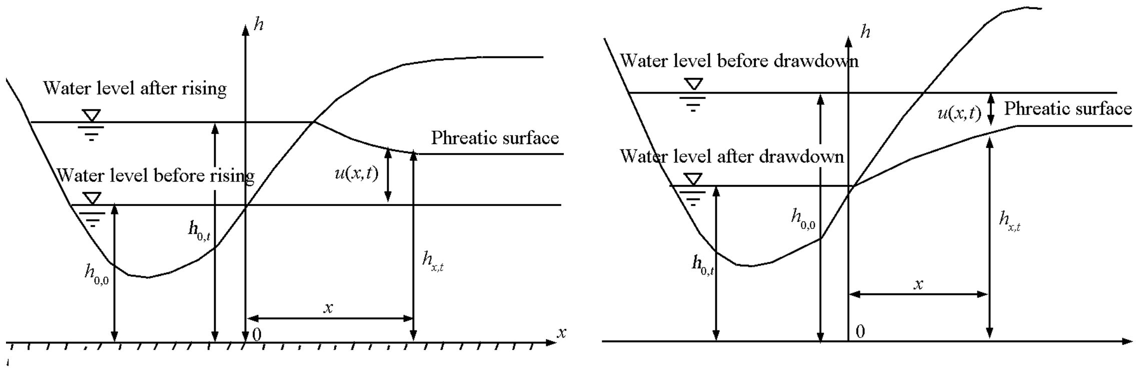


**Fig. 1 Calculation coordinates of phreatic surface**

If the water level remains unchanged after the instantaneous rising or drawdown, the amplitude of phreatic surface at the section of $x = 0$ is $u(0,t) = h_{0,t} - h_{0,0} = \Delta h_{0,t}$ after the seepage occurs. And the amplitude is $u(\infty, t) = 0$ at the section of $x = \infty$.

By converting the viable, $u(x,t) = h_{x,t} - h_{0,0}$, the unstable seepage of the underground water which remains unchanged after instantaneous rising or drawdown in the semi-infinite aquifer can be induced according to Eq. (2) to Eq. (4) as the following:

$$\begin{cases} \dfrac{\partial u}{\partial t} = a\dfrac{\partial^2 u}{\partial x^2} & 0 < x < \infty,\ t > 0 \quad (5) \\ u(x,0) = 0 & 0 < x < \infty \quad (6) \\ u(0,t) = \Delta h_{0,t} & t > 0 \quad (7) \\ u(\infty,t) = 0 & t > 0 \quad (8) \end{cases}$$

In the expression, $a = \frac{kh_m}{\mu}$ is conductivity factor.

## 2.2 The solution of mathematical model

Converting the variable $t$ in the mathematical model by Laplace.

$$\bar{u} = \int_0^\infty u\exp(-pt)\,dt \tag{9}$$

Eq. (9) could be multiplied by exp $(-pt)$ on the both sides. Then integrate $t$ in $0 \sim \infty$ as the following.

$$\int_0^\infty \frac{\partial u}{\partial t}\exp(-pt)\,dt = a\int_0^\infty \frac{\partial^2 u}{\partial x^2}\exp(-pt)\,dt \tag{10}$$

The left side of the equation is integrated by parts. The following can be obtained through the original conditions:

$$\int_0^\infty \frac{\partial u}{\partial t}\exp(-pt)\,dt = u\exp(-pt)\Big|_0^\infty + p\int_0^\infty u\exp(-pt)\,dt = p\bar{u} \tag{11}$$

The right side is:

$$a\int_0^\infty \frac{\partial^2 u}{\partial x^2}\exp(-pt)\,dt = a\frac{\partial^2}{\partial x^2}\left[\int_0^\infty u\exp(-pt)\,dt\right] = a\frac{\partial^2 \bar{u}(x,p)}{\partial x^2} \tag{12}$$

Converting Eq. (7) and Eq. (8) by Laplace

When $x = 0$:

$$\int_0^\infty u(x,t)\exp(-pt)\,dt = \int_0^\infty \Delta h_{0,t}\exp(-pt)\,dt = -\frac{\Delta h_{0,t}}{p}\exp(-pt)\Big|_0^\infty = \frac{\Delta h_{0,t}}{p} \tag{13}$$

When $x = \infty$:

$$\int_0^\infty u(x,t)\exp(-pt)\,dt = \int_0^\infty 0 \times \exp(-pt)\,dt = 0 \tag{14}$$

So the above mathematical model can be simplified as

$$\frac{d^2 u}{dx^2} - \frac{p}{a}\bar{u} = 0 \tag{15}$$

$$\bar{u}(0,p) = \frac{\Delta h_{0,t}}{p} \tag{16}$$

$$\bar{u}(\infty,p) = 0 \tag{17}$$

Eq. (15) is a second-order linear constant homogeneous coefficients differential equation, whose secular equation is $\gamma^2 - \frac{p}{a} = 0$ and the solution is $\gamma = \pm\sqrt{\frac{p}{a}}$. So the general solution is:

$$\bar{u}(x,p) = A\exp[(p/a)^{\frac{1}{2}}x] + B\exp[(p/a)^{-\frac{1}{2}}x] \quad (18)$$

Inducing the conditional expression with fixed solutions (16) and (17) into the above equation, the result is:

$$A = 0, \quad B = \frac{\Delta h_{0,t}}{p}$$

And inducing $A$ and $B$ into Eq. (18), the result is:

$$\bar{u} = \frac{\Delta h_{0,t}}{p}\exp[-(p/a)^{\frac{1}{2}}x] = \frac{\Delta h_{0,t}}{p}\exp(-\alpha p^{\frac{1}{2}}), \alpha = x/a^{\frac{1}{2}} \quad (19)$$

At last converting inversely Eq. (19) by Laplace, the following can be achieved:

$$u = \mathrm{L}^{-1}[\bar{u}] = \Delta h_{0,t}\mathrm{L}^{-1}[\frac{1}{p}e^{-\alpha x}] = \Delta h_{0,t}\mathrm{erfc}(\frac{\alpha}{2\sqrt{t}}) \quad (20)$$

or:

$$u(x,t) = \Delta h_{0,t}\mathrm{erfc}(\lambda) \quad (21)$$

In the equation:

$$\lambda = x/2(at)^{\frac{1}{2}} = (x^2/4at)^{\frac{1}{2}} \quad (22)$$

$\mathrm{erfc}(\lambda)$ is error function complement, which can be defined as:

$$\mathrm{erfc}(\lambda) = 1 - \mathrm{erf}(\lambda) = \frac{2}{\sqrt{\pi}}\int_{\lambda}^{\infty} e^{-\beta^2}d\beta \quad (23)$$

Considering $F(\lambda) = \mathrm{erfc}(\frac{x}{2\sqrt{at}}) = \frac{2}{\sqrt{\pi}}\int_{\lambda}^{\infty} e^{-\beta^2}d\beta$, it changes in accordance with time $t$and distance $x$, which is showed in Fig. 1. So Eq. (21) can be transformed as:

$$u(x,t) = \Delta h_{0,t}F(\lambda) \quad (24)$$

In practices, which conductivity factor known, the change of phreatic surface as a result of the water level change $\Delta h_{0,t}$ at any time or distance can be obtained. First $F(\lambda)$ can be founded out in Table 1 with $\lambda = \frac{x}{2\sqrt{at}}$ and the amplitude of phreatic surface can be induced through Eq. (24). So the following can be obtained:

$$h_{x,t} = h_{0,0} + \Delta h_{0,t}F(\lambda) \quad (25)$$

**Table 1 The numerical value of $F(\lambda)$**

| $\lambda$ | $\lambda^2$ | $F(\lambda)$ | $\lambda$ | $\lambda^2$ | $F(\lambda)$ |
|---|---|---|---|---|---|
| 0.003 162 | 0.001 0 | 0.964 3 | 0.500 0 | 0.25 | 0.479 5 |
| 0.040 0 | 0.001 6 | 0.954 9 | 0.632 5 | 0.40 | 0.371 1 |
| 0.050 0 | 0.002 5 | 0.943 6 | 0.774 6 | 0.60 | 0.273 3 |
| 0.063 25 | 0.004 0 | 0.928 7 | 0.894 4 | 0.80 | 0.205 9 |
| 0.077 46 | 0.006 0 | 0.912 8 | 1.000 | 1.00 | 0.157 3 |
| 0.089 44 | 0.008 0 | 0.899 4 | 1.140 | 1.30 | 0.106 9 |
| 0.100 0 | 0.010 | 0.887 5 | 1.255 | 1.60 | 0.073 6 |
| 0.126 5 | 0.016 | 0.858 0 | 1.378 | 1.90 | 0.051 3 |
| 0.158 1 | 0.025 | 0.823 1 | 1.483 | 2.20 | 0.035 9 |
| 0.200 0 | 0.040 | 0.773 1 | 1.581 | 2.50 | 0.025 4 |
| 0.244 9 | 0.060 | 0.729 1 | 1.643 | 2.70 | 0.020 2 |
| 0.282 8 | 0.080 | 0.689 2 | 1.732 | 3.00 | 0.014 3 |
| 0.316 2 | 0.010 | 0.654 8 | 1.789 | 3.20 | 0.011 4 |
| 0.400 0 | 0.16 | 0.571 6 | | | |

It is inconvenient that direct calculation with the definition equation of $F(\lambda)$ needs integral calculus. In order to get an expression which is practical, the fitting curve (Fig. 2) can be drawn by fitting polynomials. The fitting equation is:

$$F(\lambda) = \begin{cases} 0.126\,6\lambda^5 - 0.689\,8\lambda^4 + 1.295\,5\lambda^3 - 0.603\,0\lambda^2 - 0.958\,3\lambda + 0.985\,9 & (0 \leqslant \lambda < 1.8) \\ 0.0 & (\lambda \geqslant 1.8) \end{cases} \quad (26)$$

So, Eq. (25) can be transformed into:

$$h_{x,t} = \begin{cases} h_{0,0} + \Delta h_{0,t}(0.126\,6\lambda^5 - 0.689\,8\lambda^4 + 1.295\,5\lambda^3 - 0.603\,0\lambda^2 - 0.958\,3\lambda + 0.985\,9) & (0 \leqslant \lambda < 1.8) \\ h_{0,0} & (\lambda \geqslant 1.8) \end{cases} \quad (27)$$

### 2.3 The analytic solution of phreatic surface during the change of water level

Eq. (27) is the calculation of phreatic surface when the water level rises or descends instantaneously and then remains constant. But in real project, water level does not remain constant and there must be fluctuation at uneven ratio. As it is showed in Fig. 3, non-cascade changing curve can be transformed into cascade curve by splitting time period, although the change of water level is not at an even speed.

By this method, $u_i(x,t)$ $(i = 1, ..., n)$ corresponding to $(t - t_0), (t - t_1), ..., (t - t_{n-1})$ should be worked out first as showed in Eq. (28) to Eq. (31). So the whole amplitude of phreatic surface $u(x,t)$ is added by amplitudes of respective time periods $u_i(x,t)$ $(i = 1, ..., n)$, which is showed in Eq. (32):

$$u_1 = \Delta h_1 F(\frac{x}{2\sqrt{a(t - t_0)}}) \quad (28)$$

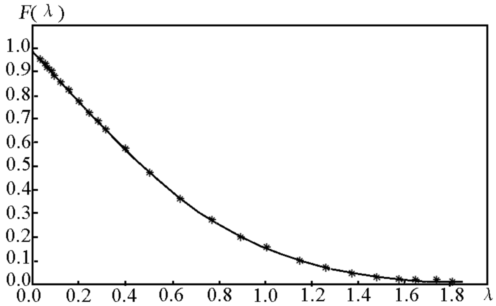


**Fig. 2 Relationship curve of $\lambda$ and $F(\lambda)$**

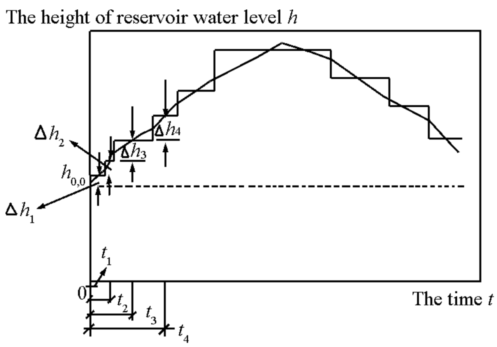


**Fig. 3 Generalizing the change of water level as cascade curve**

$$u_2 = \Delta h_2 F\left(\frac{x}{2\sqrt{a(t-t_1)}}\right) \tag{29}$$

$$u_3 = \Delta h_3 F\left(\frac{x}{2\sqrt{a(t-t_2)}}\right) \tag{30}$$

..................................

$$u_n = \Delta h_n F\left(\frac{x}{2\sqrt{a(t-t_{n-1})}}\right) \tag{31}$$

$$u = u_1 + u_2 + u_3 + \cdots + u_n = \sum_{i=1}^{n} \Delta h_i F\left(\frac{x}{2\sqrt{a(t-t_{i-1})}}\right) \tag{32}$$

The following can be got by inducing $u(x,t) = h_{x,t} - h_{0,0}$ into Eq. (32):

$$h(x,t) = h_{0,0} + \sum_{i=1}^{n} \Delta h_i F\left(\frac{x}{2\sqrt{a(t-t_{i-1})}}\right) \tag{33}$$

In the equation, $a = \frac{kh_m}{\mu}$ is conductivity factor.

Eq. (33) is the analytic solution of phreatic surface during the change of reservoir water level. By splitting $\Delta t$ in accordance with the amplitude $\Delta h_i$, the equation of analytic solution can be adopted to calculate phreatic surface with different rate of water level change.

## 3 The verification of analytic solution formula

Sand launder experiment[9] is used to verify the analytic solution formula of phreatic surface.

### 3.1 Brief introduction of sand launder experiment

The sand launder is made up by cement mortar and bricks with 3.7 m long, 1.5 m wide and 1.5 m high. On a side of the launder, there is a piezometer tube, which makes it convenient to observe and measure the water level, to determine the height of water head. The even distance between each piezometer tube is 0.3 m. On the other side of the launder, a glass window is fixed to observe the change of the phreatic surface. To drain smoothly, 5 taps are installed on a side, which makes it possible for the sand launder to sluice and drain. Having been built, the launder is filled with water and kept for 24 h to ensure that it does not leak. After the preparation, the experimental model can be constructed in the launder, which is showed in Fig. 4.

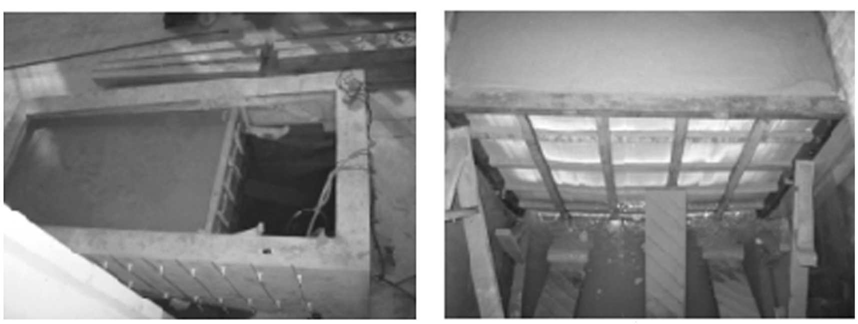

**Fig. 4 Sand Launder experiment**

The experiment is carried out step by step as the following:

1) Built a retaining structure made up by wood frame and gauze in the launder so as to hinder soil and make water pass though.

2) Fill some infiltration material in the launder hierarchically with 300 mm for each layer. The model is constructed by tight layers.

3) Turn on the feed valve and instill water into the launder till the water submerges the model. After some time, water in the launder will infiltrate into the model so that the water level will descend. So add water again to keep the water level the same height with the model.

4) Drain water by pump or tap and record the water head level of different piezometer tubes at different time.

The experiment is carried out on bigger sand model with high filtration coefficient and smaller sand-clay model with low coefficient.

### 3.2 The result and analysis of sand model experiment

The experiment on sandy clay is carried out according to the methods mentioned above. Fig. 5 displays the model.

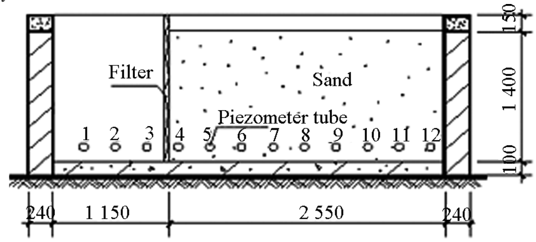


**Fig. 5 Sand model**

Since the filtration coefficient of sand model is high, the fall in water level is made respectively by one pump and two pumps. The contrastive analysis of experimental value and value of analytic formula can be found in Table 2 and Table 3.

**Table 2 Contrastive analysis of experimental value and value of analytic formula with one pump**

| Time/min | Water level/m | Calculation items | The number of piezometer tubes | | | | | | | | |
|---|---|---|---|---|---|---|---|---|---|---|---|
| | | | 4 | 5 | 6 | 7 | 8 | 9 | 10 | 11 | 12 |
| 0 | 1.400 | Initial value/m | 1.400 | 1.400 | 1.400 | 1.400 | 1.400 | 1.400 | 1.400 | 1.400 | 1.400 |
| | | Experimental value/m | 1.193 | 1.245 | 1.273 | 1.286 | 1.296 | 1.303 | 1.308 | 1.311 | 1.312 |
| 5 | 1.182 | Calculation value/m | 1.211 | 1.265 | 1.295 | 1.309 | 1.321 | 1.329 | 1.335 | 1.338 | 1.339 |
| | | Inaccuracy/% | -1.51 | -1.61 | -1.73 | -1.79 | -1.93 | -2.00 | -2.06 | -2.06 | -2.06 |
| | | Experimental value/m | 1.009 | 1.141 | 1.198 | 1.223 | 1.240 | 1.252 | 1.260 | 1.265 | 1.267 |
| 10 | 0.972 | Calculation value/m | 1.024 | 1.159 | 1.218 | 1.244 | 1.264 | 1.277 | 1.286 | 1.291 | 1.293 |
| | | Inaccuracy/% | -1.49 | -1.58 | -1.67 | -1.72 | -1.94 | -1.99 | -2.06 | -2.06 | -2.05 |
| | | Experimental value/m | 0.840 | 1.033 | 1.126 | 1.167 | 1.192 | 1.208 | 1.220 | 1.227 | 1.230 |
| 15 | 0.795 | Calculation value/m | 0.858 | 1.062 | 1.164 | 1.212 | 1.239 | 1.256 | 1.269 | 1.276 | 1.279 |
| | | Inaccuracy/% | -2.14 | -2.81 | -3.37 | -3.86 | -3.94 | -3.97 | -4.02 | -3.99 | -3.98 |
| | | Experimental value/m | 0.668 | 0.888 | 1.034 | 1.107 | 1.145 | 1.167 | 1.182 | 1.191 | 1.195 |
| 20 | 0.627 | Calculation value/m | 0.683 | 0.911 | 1.063 | 1.139 | 1.179 | 1.202 | 1.218 | 1.227 | 1.231 |
| | | Inaccuracy/% | -2.25 | -2.59 | -2.80 | -2.89 | -2.97 | -3.00 | -3.05 | -3.02 | -3.01 |

**Table 3 Contrastive analysis of experimental value and value of analytic formula with two pumps**

| Time/min | Water level/m | Calculation items | The number of piezometer tubes | | | | | | | | |
|---|---|---|---|---|---|---|---|---|---|---|---|
| | | | 4 | 5 | 6 | 7 | 8 | 9 | 10 | 11 | 12 |
| 0 | 1.400 | Initial value/m | 1.400 | 1.400 | 1.400 | 1.400 | 1.400 | 1.400 | 1.400 | 1.400 | 1.400 |
| | | Experimental value/m | 1.175 | 1.240 | 1.274 | 1.292 | 1.304 | 1.313 | 1.322 | 1.326 | 1.327 |
| 3 | 1.160 | Calculation value/m | 1.186 | 1.253 | 1.288 | 1.307 | 1.319 | 1.328 | 1.337 | 1.342 | 1.343 |
| | | Inaccuracy/% | -0.94 | -1.05 | -1.10 | -1.16 | -1.15 | -1.14 | -1.13 | -1.21 | -1.21 |
| | | Experimental value/m | 1.012 | 1.146 | 1.202 | 1.227 | 1.244 | 1.256 | 1.267 | 1.272 | 1.275 |
| 6 | 0.905 | Calculation value/m | 1.025 | 1.168 | 1.232 | 1.262 | 1.281 | 1.293 | 1.305 | 1.310 | 1.313 |
| | | Inaccuracy/% | -1.28 | -1.92 | -2.50 | -2.85 | -2.97 | -2.95 | -3.00 | -2.99 | -2.98 |
| | | Experimental value/m | 0.747 | 1.030 | 1.129 | 1.167 | 1.191 | 1.207 | 1.223 | 1.230 | 1.234 |
| 9 | 0.665 | Calculation value/m | 0.760 | 1.056 | 1.164 | 1.209 | 1.237 | 1.255 | 1.271 | 1.279 | 1.283 |
| | | Inaccuracy/% | -1.74 | -2.52 | -3.10 | -3.59 | -3.86 | -3.98 | -3.92 | -3.98 | -3.97 |
| | | Experimental value/m | 0.491 | 0.860 | 1.045 | 1.111 | 1.144 | 1.166 | 1.185 | 1.194 | 1.198 |
| 12 | 0.420 | Calculation value/m | 0.500 | 0.884 | 1.082 | 1.156 | 1.191 | 1.214 | 1.234 | 1.243 | 1.247 |
| | | Inaccuracy/% | -1.83 | -2.79 | -3.54 | -4.05 | -4.11 | -4.12 | -4.14 | -4.10 | -4.09 |

### 3.3 The result and analysis of sand-clay model experiment

Some clay is added into sand to reduce the filtration coefficient and change the character of filtration of sad. The ratio of sand to clay is 1∶3. Water is drained out respectively by one tap and two taps because the filtration coefficient is low. The contrastive analysis of experiment value and calculation value of analytic expression is displayed in Table 4 and Table 5.

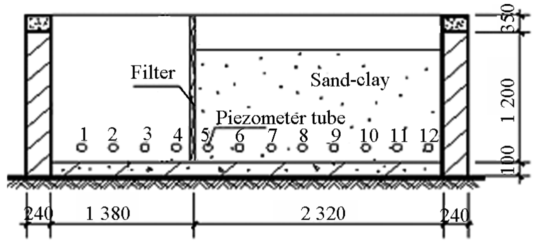


**Fig.6 Sand-clay model**

**Table 4 Contrastive analysis of experimental value and value of analytic formula with one tap**

| Time/min | Water level/m | Calculation items | The number of piezometer tubes | | | | | | | |
|---|---|---|---|---|---|---|---|---|---|---|
| | | | 5 | 6 | 7 | 8 | 9 | 10 | 11 | 12 |
| 0 | 1.200 | Initial value/m | 1.200 | 1.200 | 1.200 | 1.200 | 1.200 | 1.200 | 1.200 | 1.200 |
| | | Experimental value/m | 1.127 | 1.133 | 1.137 | 1.141 | 1.143 | 1.145 | 1.146 | 1.147 |
| 1 | 1.120 | Calculation value/m | 1.145 | 1.151 | 1.156 | 1.160 | 1.162 | 1.163 | 1.165 | 1.166 |
| | | Inaccuracy/% | −1.60 | −1.59 | −1.67 | −1.67 | −1.66 | −1.57 | −1.66 | −1.66 |
| | | Experimental value/m | 1.072 | 1.085 | 1.095 | 1.103 | 1.108 | 1.113 | 1.115 | 1.117 |
| 2 | 1.040 | Calculation value/m | 1.090 | 1.106 | 1.117 | 1.125 | 1.129 | 1.130 | 1.131 | 1.132 |
| | | Inaccuracy/% | −1.68 | −1.94 | −2.01 | −1.99 | −1.90 | −1.53 | −1.43 | −1.34 |
| | | Experimental value/m | 1.025 | 1.044 | 1.059 | 1.070 | 1.078 | 1.084 | 1.089 | 1.091 |
| 3 | 0.965 | Calculation value/m | 1.043 | 1.063 | 1.084 | 1.098 | 1.117 | 1.119 | 1.120 | 1.121 |
| | | Inaccuracy/% | −1.76 | −1.82 | −2.36 | −2.62 | −3.62 | −3.23 | −2.85 | −2.75 |
| | | Experimental value/m | 0.987 | 1.007 | 1.025 | 1.040 | 1.051 | 1.059 | 1.065 | 1.068 |
| 4 | 0.890 | Calculation value/m | 1.008 | 1.030 | 1.051 | 1.063 | 1.069 | 1.071 | 1.072 | 1.073 |
| | | Inaccuracy/% | −2.13 | −2.28 | −2.54 | −2.21 | −1.71 | −1.13 | −0.66 | −0.47 |

**Table 5 Contrastive analysis of experimental value and value of analytic formula with two taps**

| Time/min | Water level/m | Calculation items | The number of piezometer tubes | | | | | | | |
|---|---|---|---|---|---|---|---|---|---|---|
| | | | 5 | 6 | 7 | 8 | 9 | 10 | 11 | 12 |
| 0 | 1.200 | Initial value/m | 1.200 | 1.200 | 1.200 | 1.200 | 1.200 | 1.200 | 1.200 | 1.200 |
| | | Experimental value/m | 1.076 | 1.092 | 1.103 | 1.111 | 1.117 | 1.122 | 1.126 | 1.127 |
| 1 | 1.049 | Calculation value/m | 1.098 | 1.121 | 1.142 | 1.154 | 1.157 | 1.158 | 1.159 | 1.160 |
| | | Inaccuracy/% | −2.04 | −2.66 | −3.54 | −3.87 | −3.58 | −3.21 | −2.93 | −2.93 |
| | | Experimental value/m | 1.006 | 1.029 | 1.048 | 1.062 | 1.073 | 1.081 | 1.088 | 1.091 |
| 2 | 0.900 | Calculation value/m | 1.036 | 1.057 | 1.076 | 1.082 | 1.087 | 1.090 | 1.092 | 1.093 |
| | | Inaccuracy/% | −2.98 | −2.72 | −2.67 | −1.88 | −1.30 | −0.83 | −0.37 | −0.18 |
| | | Experimental value/m | 0.957 | 0.980 | 1.003 | 1.022 | 1.036 | 1.047 | 1.056 | 1.061 |
| 3 | 0.762 | Calculation value/m | 0.995 | 1.035 | 1.054 | 1.065 | 1.074 | 1.076 | 1.077 | 1.078 |
| | | Inaccuracy/% | −3.97 | −2.78 | −5.08 | −4.21 | −3.67 | −2.77 | −1.99 | −1.60 |
| | | Experimental value/m | 0.913 | 0.937 | 0.964 | 0.987 | 1.004 | 1.017 | 1.029 | 1.034 |
| 4 | 0.630 | Calculation value/m | 0.957 | 0.978 | 0.991 | 1.002 | 1.011 | 1.014 | 1.015 | 1.016 |
| | | Inaccuracy/% | −4.82 | −4.38 | −2.80 | −1.52 | −0.70 | 0.29 | 1.36 | −1.93 |

According to Table 2 to Table 5, the calculation value of analytic expression is a bit much more than the experimental value and the inaccuracy is no more than 5 % generally except for some points, which increases as the water level descends. As the horizon distance increases after the water descends to a level, the inaccuracy becomes larger and the location of phreatic surface in the rear of the slope does not change dramatically. Through these results of these two experiments, the analytic solution has higher calculation accuracy than that in the Ref. [9] since it has taken the influence of the changing ratio of the water level into consideration.

## 4 Contrastive analysis of analytic solution, numerical solution and experiential generalizing

The seepage module of ground water of PLAXFLOW is adopted to further test the correctness of analytic solution and contrast with the solution of experiential generalizing.

In real projects, technicians from different departments often generalize through experiences in different methods. Some regard the line between the water far away the reservoir slope and the ultimate water after change as the location of phreatic surface; some take the initial water level as the phreatic surface; and the others choose the one-third of the height of the sliding mass. Here the first method is used as the solution of experiential generalizing to compare with the numerical solution and analytic solution.

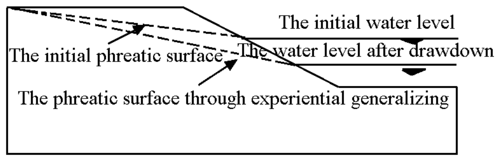


**Fig. 7 The phreatic surface through experiential generalizing**

Example: as showed in Fig. 8, the grading angle is 45°; the filtration coefficient of the soil is $k_x = k_y = 0.005$ m/d; the water in the front of the slope descends at the speed of 3 m/d by 15 m; the rear slope is the constant water head boundary and $h = 15$ m.

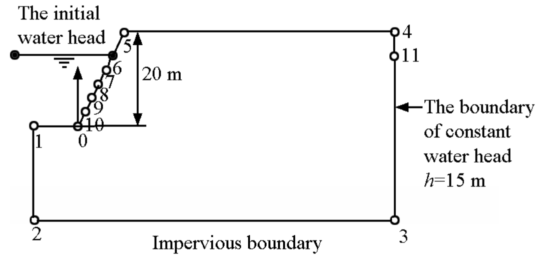


**Fig. 8 Calculation model**

In Fig. 9, the locations of phreatic surface of different time are displayed, which are acquired by instantaneous analysis of seepage module of underground water through PLAXFLOW.

Table 6 illustrates the comparison of analytic solution, numerical solution and the solution of experiential generalizing, whose inaccuracy is compared by the numerical solution at the same level.

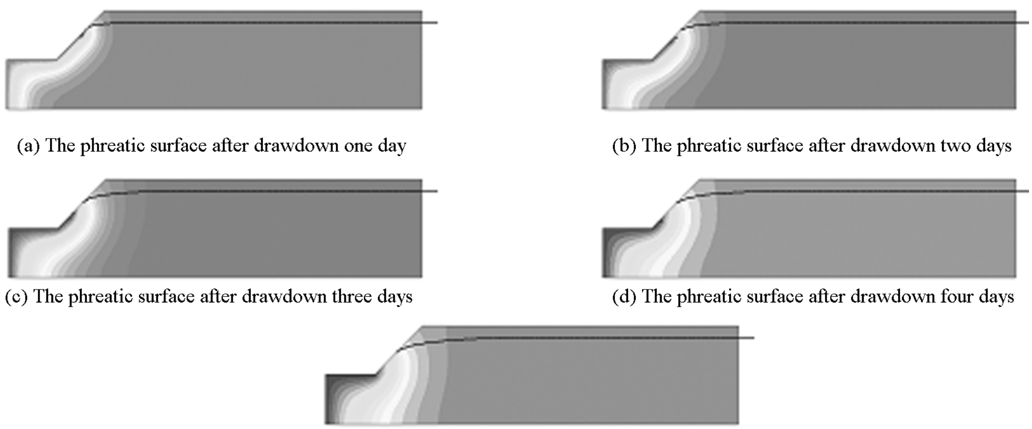

(a) The phreatic surface after drawdown one day
(b) The phreatic surface after drawdown two days
(c) The phreatic surface after drawdown three days
(d) The phreatic surface after drawdown four days
(e) The phreatic surface after drawdown five days

**Fig. 9 The locations of phreatic surface of different time**

**Table 6 The calculation results of phrestic surface**
**(a) The height of phreatic surface after drawdown one day**

| Calculation methods | Horizontal distance/m | | | | | | | | | | | | Remarks |
|---|---|---|---|---|---|---|---|---|---|---|---|---|---|
| | 0 | 10 | 20 | 30 | 40 | 50 | 60 | 70 | 90 | 110 | 130 | 150 | Coordinates of spill point |
| Numerical solution | 0.0 | 10.0 | 14.6 | 14.9 | 15.0 | 15.0 | 15.0 | 15.0 | 15.0 | 15.0 | 15.0 | 15.0 | (12.1,12.1) |
| Analytic solution | 0.0 | 10.0 | 14.1 | 14.3 | 14.4 | 14.5 | 14.6 | 14.8 | 14.9 | 14.9 | 14.9 | 15.0 | (12.0,12.0) |
| Inaccuracy/% | 0.0 | 0.0 | −3.42 | −4.03 | −4.00 | −3.33 | −2.67 | −1.33 | −0.67 | −0.67 | −0.67 | 0.0 | (−0.8, −0.8) |
| The solution of experiential generalizing | 0.0 | 10.0 | 12.2 | 12.4 | 12.6 | 12.8 | 13.0 | 13.3 | 13.7 | 14.1 | 14.6 | 15.0 | (12.0,12.0) |
| Inaccuracy/% | 0.0 | 0.0 | −16.4 | −16.8 | −16.0 | −14.7 | −13.3 | −11.3 | −8.7 | −6.0 | −2.7 | 0.0 | (−0.8, −0.8) |

(b) **The height of phreatic surface after drawdown three days**

| Calculation methods | Horizontal distance/m | | | | | | | | | | | | Remarks |
|---|---|---|---|---|---|---|---|---|---|---|---|---|---|
| | 0 | 10 | 20 | 30 | 40 | 50 | 60 | 70 | 90 | 110 | 130 | 150 | Coordinates of spill point |
| Numerical solution | 0.0 | 10.0 | 13.7 | 14.5 | 14.8 | 14.9 | 15.0 | 15.0 | 15.0 | 15.0 | 15.0 | 15.0 | (10.5,10.5) |
| Analytic solution | 0.0 | 10.0 | 12.7 | 14.5 | 14.8 | 14.8 | 14.9 | 14.9 | 15.0 | 15.0 | 15.0 | 15.0 | (10.1,10.1) |
| Inaccuracy/% | 0.0 | 0.0 | -7.30 | 0.0 | 0.0 | -0.67 | -0.67 | -0.67 | 0.0 | 0.0 | 0.0 | 0.0 | (-3.81, -3.81) |
| The solution of experiential generalizing | 0.0 | 6.3 | 6.9 | 7.5 | 8.1 | 8.8 | 9.4 | 10.0 | 11.3 | 12.5 | 13.8 | 15.0 | (6.0,6.0) |
| Inaccuracy/% | 0.0 | -37.0 | -49.6 | -48.3 | -45.3 | -40.9 | -37.3 | -33.3 | -24.7 | -16.7 | -8.0 | 0.0 | (-42.9, -42.9) |

(c) **The height of phreatic surface after drawdown five days**

| Calculation methods | Horizontal distance/m | | | | | | | | | | | | Remarks |
|---|---|---|---|---|---|---|---|---|---|---|---|---|---|
| | 0 | 10 | 20 | 30 | 40 | 50 | 60 | 70 | 90 | 110 | 130 | 150 | Coordinates of spill point |
| Numerical solution | 0.0 | 9.7 | 12.7 | 13.9 | 14.5 | 14.7 | 14.9 | 15.0 | 15.0 | 15.0 | 15.0 | 15.0 | (8.9,8.9) |
| Analytic solution | 0.0 | 9.2 | 11.8 | 13.5 | 13.9 | 14.3 | 14.7 | 14.8 | 14.8 | 14.9 | 14.9 | 15.0 | (8.6,8.6) |
| Inaccuracy/% | 0.0 | -5.15 | -7.09 | -2.88 | -4.14 | -2.72 | -1.34 | -1.33 | -1.33 | -0.67 | -0.67 | 0.0 | (-3.37, -3.37) |
| The solution of experiential generalizing | 0.0 | 1.0 | 2.0 | 3.0 | 4.0 | 5.0 | 6.0 | 7.0 | 9.0 | 11.0 | 13.0 | 15.0 | (0.0,0.0) |
| Inaccuracy/% | 0.0 | -89.7 | -84.3 | -78.4 | -72.4 | -66.0 | -59.7 | -53.3 | -40.0 | -26.7 | -13.3 | 0.0 | (-100.0, -100.0) |

It can be concluded through Table 6 that the results of analytic solution and numerical solution are similar. However the inaccuracy of the solution of experiential generalizing is larger comparatively. The more water level drawdown is, the bigger inaccuracy is, which reaches 80 % in the front of the slope. As a result, the analytic solution and numerical solution acquired by instantaneous analysis of seepage module of underground water through PLAXFLOW are dependable and can reflect the hysteresis effect of the change of the phreatic surface. In Table 6 the spilling points of the phreatic surface according to numerical solution and analytic solution are higher than the water level in the front of the slope, which displays the hysteresis effect. If experiential generalizing is applied to analyze the slope stability, such as the slope of reservoir bank in the Three Gorges area, the potential dangers would be caused to people's life and property.

## 5 Conclusions

While deducing the analytic solution of the phreatic surface in the slope of reservoir bank, we assume the water level mostly change at a constant speed $V_0$, which does not correspond to the actual situation. So in this paper, the analytic solution of phreatic surface is further studied and the following conclusions can be drawn:

1) By inducing the change of water level $\Delta h_i$ during the period of $\Delta t$ (if water ascends, $\Delta h_i > 0$; if water descends, $\Delta h_i < 0$; if water remains still, $\Delta h_i = 0$). As a result, if $\Delta t$ (the time during which $\Delta h_i$ takes place) is split, analytic solution is suitable to locate the phreatic surface on the condition that water level changes at a changing rate.

2) The correctness of analytic solution is tested through the model of sand and sand-clay, which shows the calculation results of analytic solution are larger than the experiential value and the inaccuracy is no more than 5 %. In addition, the inaccuracy increases as the water level descends. As the horizon distance increases after the water descends to a level, the inaccuracy becomes larger and the location of phreatic surface in the slope rear does not change dramatically.

3) The numerical solution of the phreatic surface, which is acquired by underground water seepage module of PLAXFLOW, is compared with analytic solution. It can be concluded that these two results are close to each other and the hysteresis effect can be illustrated during the drawdown of the water level.

4) By comparing the results of analytic solution, numerical solution and the solution of experiential generalizing, the inaccuracy of experiential generalizing is evident and will become larger as the water descends even exceed 80 %. So if the method of experiential generalizing is adopted in the slope of reservoir bank in the Three Gorges area, it will result in many potential dan-

gers even geological disasters.

## References


[1] U S Army Corps of Engineers. Engineering and Design – Stability of Earth and Rock Fill Dams[S]. Office of the Chief of Engineers, U S Army Corps of Engineers, Department of the Army, Engineering Manual EM, 1110-1902, 1970.

[2] Chen Zuyu. The calculation steps of overall stress method in the earth and rockfill dam slope stability analysis during the pelter of reservoir water level[J]. Water Resources and Hydropower Engineering,1985, (9):30-32.

[3] Schnitter G, Zeller J. The seepage caused by the fluctuation of reservoir water level in the fill dam[J]. Canadian Geotechnical Journal, 1988, (5):33-36.

[4] Zhu Wei, Qin Jianshe, Gao Yufeng. Analytic method to solve initial phreatic level for unsaturated embankments[J]. Journal of Hohai University (Natural Sciences), 2003, 31, (3):314-317.

[5] Liu Xinxi. Effects of drawdown of reservoir water level on landslide stability[D]. Wuhan: China University of Geosciences, 2003.

[6] Shi Weimin, Zheng Yingren. Analysis on stability of landslide during reservoir drawdown[J]. Journal of Hydraulic Engineering, 2004, (3):76-80.

[7] Feng Wenkai, Shi Yuchuan, Chai Hejun, et al. The simplified solution of phreatic saturation line under the actions of rainfall and reservoir water level fluctuation[J]. Journal of Chengdu University of Technology(Science & Technology Edition), 2006, 23(1):90-94.

[8] Chen Chongxi, Lin Min. Underground Hydrodynamics[M]. Wuhan: China University of Geosciences Press, 1999.

[9] Shi Weimin. The research on the practical method to analyzing the landslide and slope stability in the Three Gorges reservoir area [D]. Chongqing: Logistic Engineering University, 2004.


## Author


Tang Xiaosong, male, born in 1979, graduated from Logistical Engineering University and obtained doctor's degree. Mr. Tang has published 12 papers. His current research is stability analysis on geological engineering. He can be reached by E-mail: hnm97@163.com


---

(cont. from p. 68)

## Author


Zhang Daobing, male, was born in 1977 and graduated from Hunan University of Science and Technology with a master's degree in 2007. Now he works in the School of Energy & Safety Engineering as a lecturer at Hunan University of Science and Technology. Mr. Zhang has published 10 papers. His current research is mining systems engineering and structure reliability etc. He can be reached by E-mail: dbzhang@hnust.edu.cn



Foundation item: Supported by a grant from the National Natural Science Foundation of China (No. 50674046) and a grant from the Scientific Research Fund of Hunan Provincial Education Department(No. 07C293).